Solid State Structures and Phosphine Exchange Reactions of (1-Me-Indenyl)(PR_3)Ni−Cl

Frédéric-Georges Fontaine, Marc-André Dubois, and Davit Zargarian*

Département de Chimie, Université de Montréal, Montréal (Québec), Canada H3C 3J7

Received July 9, 2001

The complexes (1-Me-Ind)(PR_3)Ni−Cl (Ind = indenyl; R = Me (**2**), Cy (**3**), Bu (**4**), and $(CH_2)_2(CF_2)_5CF_3$ (**5**)) have been prepared by the direct reaction of the corresponding $(PR_3)_2NiCl_2$ with Li(1-Me-Ind) or via phosphine exchange reactions with (1-Me-Ind)(PR'_3)Ni−Cl (R′ = Ph (**1**) and Me). Solution NMR and single-crystal X-ray diffraction studies of the structures of **2** and **3** have allowed an analysis of the mode of coordination of the 1-Me-Ind ligand both in the solid state and in solution. Kinetic studies have shown that the substitution of PPh_3 in (1-Me-Ind)(PPh_3)Ni−Cl by PCy_3 follows a second-order rate (associative mechanism) with the following kinetic parameters: K_2 ($\times 10^{-2}$ M^{-1} s^{-1}) = 1.1 ± 0.1 at 233 K, 1.9 ± 0.4 at 245 K, 15 ± 2 at 284 K, 21 ± 2 at 293 K, and 34 ± 7 at 303 K; $\Delta H^{\ddagger} = 6.40 \pm 0.07$ kcal/mol; $\Delta S^{\ddagger} = -40 \pm 4$ eu. The implications of these results for the mechanisms of the polymerization reactions catalyzed by these complexes have been discussed.

Introduction

Recent reports have documented the emergence of a number of Ni(II) compounds that act as effective precatalysts for the polymerization of ethylene and other α-olefins.[1] Notable among these are the complexes (η^2-(N,O)-salicylaldimine)Ni(PPh_3)(Ar) and (α-diimine)NiX_2 (X = Br, Me). Brookhart et al. have shown[2] that the polymerization catalysis in the latter system proceeds via a cationic mechanism, whereas Grubbs et al. have shown[3] that the salicylaldimine system follows a noncationic pathway involving the predissociation of PPh_3.

In this context, we have reported that the complexes (Ind′)(PR_3)Ni−X (Ind′ = indenyl and its substituted derivatives; R = Ph, Me, Cy; X = Cl, Me, CC−Ph)[4] act as precatalysts in a number of oligomerization[5] and polymerization[6] reactions, including the polymerization of ethylene.[6b] The results of mechanistic experiments have led us to conclude that the polymerization of ethylene in this system involves noncationic intermediates as in the Grubbs system; unlike the Grubbs system, however, the PR_3 ligand in our complexes remains coordinated to the Ni center during the catalysis. Indeed, higher catalytic activities were displayed by complexes bearing more strongly coordinating phosphines.[7]

As a follow-up to the polymerization studies mentioned above, we have studied the structural features of some of these precatalysts with a view to finding structure−activity relationships; in addition, we have examined the phosphine exchange reactions in these complexes in order to probe the likelihood of phosphine dissociation reactions similar to those reported for the Grubbs systems. The present paper reports the preparation and characterization of the complexes (1-Me-Ind)(PR_3)Ni−Cl (R = Me (**2**), Cy (**3**), Bu (**4**), and $(CH_2)_2(CF_2)_5CF_3$ (**5**)), including the solid state structures of the PMe_3 and PCy_3 derivatives, and describes the results of a kinetic study on the ligand exchange reaction between (1-Me-Ind)(PPh_3)Ni−Cl, **1**, and PCy_3.

Experimental Section

General Comments. All manipulations were performed under an inert atmosphere of N_2 or argon using standard Schlenk techniques and a drybox. Dry, oxygen-free solvents were employed throughout. The synthesis of (1-Me-Ind)(PPh_3)Ni−Cl, **1**, has been reported previously;[4b] $(PMe_3)_2NiCl_2$ was prepared from $NiCl_2$ and PMe_3. The reagent $P\{(CH_2)_2(CF_2)_5CF_3\}_3$ was donated by Dr. I. Horvath; all other reagents used in the experiments were obtained from commercial sources and used as received. The elemental analyses were performed by the Laboratoire d'Analyse Élémentaire (Université de Montréal). The NMR spectra were recorded using the following spectrometers: Bruker AMX400 (^1H at 400 MHz, $^{13}C\{^1H\}$ at 100.56 MHz, and $^{31}P\{^1H\}$ at 161.92 MHz) and Bruker AV300 (^1H at 300 MHz).

(1-Me-Ind)(PMe_3)Ni−Cl (2). A THF solution (130 mL) of Li(1-Me-Ind) (477 mg, 3.5 mmol) was added dropwise to a

(1) Bauers, F. M.; Mecking, S. *Macromolecules* **2001**, *34*, 1165, and references therein.

(2) (a) Johnson, L. K.; Killian, C. M.; Brookhart, M. *J. Am. Chem. Soc.* **1995**, *117*, 6414. (b) Johnson, L. K.; Killian, C. M.; Arthur, S. D.; Feldman, J.; McCord, E.; McLain, S. J.; Kreutzer, K. A.; Bennett, M. A.; Coughlin, E. B.; Ittel, S. D.; Parthasarathy, A.; Tempel, D.; Brookhart, M. (UNC−Chapel Hill/DuPont) PCT Int. Patent WO 96/23010, 1996; *Chem. Abstr.* **1996**, *125*, 222773t. (c) Svejda, S. A.; Johnson, L. K.; Brookhart, M. *J. Am. Chem. Soc.* **1999**, *121*, 10634, and references therein.

(3) Younkin, T. R.; Connor, E. F.; Henderson, J. I.; Friedrich, S. K.; Grubbs, R. H.; Bansleben, D. A. *Science* **2000**, *287*, 460, and references therein.

(4) (a) Dubuc, I.; Dubois, M.-A.; Bélanger-Gariépy, F.; Zargarian, D. *Organometallics* **1999**, *18*, 30. (b) Huber, T. A.; Bayrakdarian, M.; Dion, S.; Dubuc, I.; Bélanger-Gariépy, F.; Zargarian, D. *Organometallics* **1997**, *16*, 5811. (c) Bayrakdarian, M.; Davis, M. J.; Reber, C.; Zargarian, D. *Can. J. Chem.* **1996**, *74*, 2194. (d) Huber, T. A.; Bélanger-Gariépy, F.; Zargarian, D. *Organometallics* **1995**, *14*, 4997.

(5) Fontaine, F.-G.; Kadkhodazadeh, T.; Zargarian, D. *J. Chem. Soc., Chem. Commun.* **1998**, 1253.

(6) (a) Wang, R.; Bélanger-Gariépy, F.; Zargarian, D. *Organometallics* **1999**, *18*, 5548. (b) Dubois, M.-A.; Wang, R.; Zargarian, D.; Tian, J.; Vollmerhaus, R.; Li, Z.; Collins, S. *Organometallics* **2001**, *20*, 663.

(7) For example, the PMe_3 and PCy_3 derivatives are almost an order of magnitude more active in the polymerization of ethylene in comparison to the PPh_3 analogue (ref 6b).

10.1021/om010608w CCC: $20.00
Publication on Web 10/30/2001

stirring THF solution (40 mL) of Ni(PMe$_3$)$_2$Cl$_2$ (1.0 g, 3.5 mmol) which was kept at 60 °C. During the addition, the reaction vessel was placed under dynamic vacuum for a few seconds every 10 min in order to remove the free PMe$_3$ liberated by the reaction. The final mixture was stirred for 30 min and then evaporated to give a red powder (940 mg, crude yield 90%). Recrystallization from Et$_2$O/hexanes gave 420 mg of dark red crystals (40% yield). ^{1}H NMR (C_6D_6): δ 7.05 (d, $^3J_{H-H}$ = 7.6, H7), 6.98 (t, $^3J_{H-H}$ = 7.2, H5 or H6), 6.90 (t, $^3J_{H-H}$ = 7.3, H5 or H6), 6.55 (d, $^3J_{H-H}$ = 7.3, H4), 6.11 (d, $^3J_{H-H}$ = 2.6, H2), 3.58 (br, H3), 1.61 (d, $^4J_{H-P}$ = 2.6, Ind-CH$_3$), 0.71 (d, $^2J_{H-P}$ = 2.6, P-CH$_3$). ^{13}C{^{1}H} NMR (C_6D_6): δ 130.21 (d, $^2J_{C-P}$ = 1.4, C7a), 126.29 (C3a), 125.75, 125.47, 118.15, 116.05 (C4, C5, C6, C7), 103.77 (s, C2), 101.29 (d, $^2J_{C-P}$ = 16.6, C1), 59.53 (C3), 14.68 (d, $^1J_{C-P}$ = 28.4, P-CH$_3$), 11.97 (d, $^3J_{C-P}$ = 2.8, Ind-CH$_3$). ^{31}P{^{1}H} NMR (C_6D_6): δ −10.61 (s). Anal. Calcd for $C_{13}H_{18}Ni_1P_1Cl_1$: C, 52.15; H, 6.06. Found: C, 51.70; H, 6.24.

(1-Me-Ind)Ni(PCy$_3$)Cl (3). A solution of (1-Me-Ind)(PMe$_3$)Ni−Cl (400 mg, 1.34 mmol) and PCy$_3$ (376 mg, 1.34 mmol) in Et$_2$O (40 mL) was stirred for 2 h. Evaporation of the solvent followed by an EtOH washing gave a red powder (400 mg, 59%); single crystals suitable for X-ray studies and elemental analysis were obtained by recrystallization from cold hexanes. ^{1}H NMR (C_6D_6): δ 7.01, 6.86 (br s, H4/H7, H5/H6), 6.33 (s, H2), 4.11 (s, H3), 1.94−1.10 (m, PCy$_3$); the signal for Ind-CH$_3$ was obscured by PCy$_3$ signals. ^{13}C{^{1}H} NMR (C_6D_6): δ 129.72 (d, $^2J_{C-P}$ = 2.8, C7a), 127.34 (C3a), 123.10, 121.67, 115.45, 115.33 (C4, C5, C6, C7), 101.30 (C2), 97.10 (d, $^2J_{C-P}$ = 12.5, C1), 55.42 (C3), 32.07 (d, $^1J_{C-P}$ = 19.4, C$_{ipso}$), 27.13 (d, $^2J_{C-P}$ = 10.4, 2 C$_{ortho}$), 24.82 (d, $^3J_{C-P}$ = 4.9, C$_{meta}$), 24.71 (d, $^3J_{C-P}$ = 4.2, C$_{meta}$), 23.65 (s, C$_{para}$) 9.34 (d, $^3J_{C-P}$ = 2.8, Ind-CH$_3$). ^{31}P-{^{1}H} NMR (C_6D_6): δ 37.17 (s). Anal. Calcd for $C_{28}H_{42}Ni_1P_1Cl_1$: C, 66.76; H, 8.40. Found: C, 66.35; H, 8.89.

(1-Me-Ind)Ni(PBu$_3$)Cl (4). Neat PBu$_3$ (165 μL, 0.66 mmol) was added via a syringe to the red solution of (1-Me-Ind)-(PMe$_3$)Ni−Cl (200 mg, 0.66 mmol) in Et$_2$O (40 mL). The resulting mixture was stirred for 2 h with periodic venting to remove the PMe$_3$ generated in the reaction. Evaporation of the solvent and extraction of the residue with hexanes (10 mL) afforded, after removal of the volatiles, a black oil (236 mg, 84% crude yield) which contained some PBu$_3$ and other unidentified impurities. Further attempts to purify this oil by recrystallization were unsuccessful. ^{1}H NMR (C_6D_6): δ 7.05 (d, $^3J_{H-H}$ = 7.6, H7), 7.00 (t, $^3J_{H-H}$ = 7.2, H5 or H6), 6.88 (d, $^3J_{H-H}$ = 7.2, H5 or H6), 6.24 (d, $^3J_{H-H}$ = 2.5, H2), 3.75 (dd, $^3J_{H-P}$ = 4.0, $^3J_{H-H}$ = 2.8, H3), 1.60 (d, $^4J_{H-P}$ = 5.4, Ind-CH_3), 1.45−1.21 (m, P(CH_2)$_3$), 0.84 (t, $^3J_{H-H}$ = 7.1, P(CH$_2$)$_3$CH_3). ^{13}C-{^{1}H} NMR (C_6D_6): δ 130.60 (C7a), 126.95 (C3a), 125.53, 125.36, 118.25, 116.43 (C4, C5, C6, C7), 103.93 (C2), 101.11 (d, $^2J_{C-P}$ = 13.2, C1), 58.72 (C3), 26.42 (CH_2CH$_3$), 24.54 (d, $^2J_{C-P}$ = 13.2, P-CHCH$_2$), 24.03 ($^1J_{C-P}$ = 24.9, P-CH_2), 14.01 (CH$_2$CH_3). ^{31}P{^{1}H} NMR (C_6D_6): δ 15.09 (s).

(1-Me-Ind)Ni{P[(CH$_2$)$_2$(CF$_2$)$_5$CF$_3$]$_3$}Cl (5). A solution of (1-Me-Ind)(PPh$_3$)Ni−Cl (485 mg, 1.0 mmol) and P{(CH$_2$)$_2$-(CF$_2$)$_5$CF$_3$}$_3$ (1.13 g, 1.05 mmol) in Et$_2$O (30 mL) was stirred for 2 h. The solvent was evaporated and the residue crystallized from a cold Et$_2$O/hexanes solution. A dark orange solid was obtained (620 mg, 48%). ^{1}H NMR (CDCl$_3$): δ 7.18 (d, $^3J_{H-H}$ = 7.8, H7), 7.14 (t, $^3J_{H-H}$ = 7.5, H5 or H6), 7.04 (t, $^3J_{H-H}$ = 7.4, H5 or H6), 6.83 (d, $^3J_{H-H}$ = 7.6, H4), 6.34 (d, $^3J_{H-H}$ = 2.6, H2), 4.25 (pt, $^3J_{H-H}$ = $^3J_{H-P}$ = 3.4, H3), 2.19, and 1.89 (m, P−CH_2CH_2), 1.53 (d, $^4J_{H-P}$ = 6.0, Ind-CH_3). ^{13}C{^{1}H} NMR (CDCl$_3$): δ 129.11 (d, $^2J_{C-P}$ = 2.1, C7a), 127.10, 127.04, 118.73, 115.98 (C4, C5, C6, C7), 125.59 (C3a), 105.54 (d, $^2J_{C-P}$ = 13.2, C1), 103.93 (C2), 60.91 (C3), 26.31 (t, $^2J_{C-F}$ = 22.4, P−CH$_2$CH_2), 15.53 (d, $^1J_{C-P}$ = 24.2, P-CH_2), 11.98 (d, $^3J_{C-P}$ = 3.5, Ind-CH$_3$); the CF$_2$ were not detected presumably because of (a) the inherently weaker intensities of signals due to quaternary C nuclei and (b) the extended $^1J_{C-F}$ and $^2J_{C-F}$ couplings arising from the diastereotopic fluorines. ^{19}F{^{1}H} NMR (CDCl$_3$): δ −82.33 (t,$^3J_{F-F}$ = 8.9, CF$_3$), −116.05 (q, $^3J_{F-F}$ = 15.2, CF_2CF$_3$), −123.43 (br, 2F), −124.46 (br, 4F), −127.72 (br, 2F). ^{31}P{^{1}H} NMR (CDCl$_3$): δ 22.08 (s). Anal. Calcd for $C_{34}H_{21}F_{39}Ni_1P_1Cl_1$: C, 31.53; H, 1.64. Found: C, 31.89; H, 1.66.

Crystal Structure Determinations. A dark red crystal of **2** was attached to a glass fiber and transferred rapidly and under a cold stream of nitrogen to an Enraf-Nonius CAD-4 diffractometer equipped with a low-temperature gas stream cryostat for data collection at 220(2) K. The data were collected with graphite-monochromated Cu Kα radiation; the refinement of the cell parameters was done using CAD-4 software[8] on 25 reflections, while NRC-2 and NRC-2A were used for the data reduction.[9] The crystal data for **3** was collected on a Bruker AXS SMART 2K diffractometer using graphite-monochromated Cu Kα radiation at 293(2) K (SMART[10] software). Cell refinement and data reduction were carried out using SAINT.[11] Both structures were solved by direct methods using SHELXS96[12] for **2** and SHELXS97[13] for **3**, and the refinements were done on F^2 by full-matrix least squares. All non-hydrogen atoms were refined anisotropically, while the hydrogens (isotropic) were constrained to the parent atom using a riding model. The procedure used to treat the twinning detected in the crystal of **2** is described in the Supporting Information. In the case of the noncentrosymmetric structure of **2**, the overall absolute structure was determined by the Flack parameter of 0.0(8).[14] Crystal data and experimental details for both compounds are listed in Table 1, and selected bond distances and angles are listed in Table 2.

Kinetic Studies. The rate of the ligand exchange reaction between (1-Me-Ind)(PPh$_3$)Ni−Cl, **1**, and PCy$_3$ was studied under pseudo-first-order conditions using a large excess of PCy$_3$. The low-temperature data were obtained using NMR spectroscopy. Toluene-d_8 solutions containing accurately measured quantities of the reactants and Ph$_3$P=O (as internal reference) were placed in high-precision NMR tubes, and the samples were cooled to the required temperature (245 and 233 K) inside the spectrometer probe. The gradually decreasing intensity of the ^{31}P{^{1}H} signal for **1** was monitored vs time, and the values of [**1**] were determined relative to [Ph$_3$P=O]. Plots of ln([**1**]/[**1**]$_0$) vs time gave straight lines passing through the origin with slopes of k_{obs}, while plots of the k_{obs} values vs different [PCy$_3$]$_0$ (10-, 15-, and 20-fold excess) gave straight lines with slopes of K_2. The rates of the exchange reaction at high temperatures were determined by UV−vis spectroscopy. (The electronic spectra of this family of complexes have been reported previously.[4c]) Thus, the time course of the absorbance was monitored at 412 nm, and the data were subjected to a least-squares analysis in order to obtain the pseudo-first-order rate constants, k_{obs}. Plotting the k_{obs} values vs different [PCy$_3$]$_0$ (10-, 15-, 20-, and 25-fold excess; [**1**]$_0$ = 1.1 × 10^{-3} M) gave straight lines with slopes of K_2. The activation parameters $\Delta H^{\ddagger}$ and $\Delta S^{\ddagger}$ were obtained from a plot of ln(K_2/T) vs 1/T (Figure 3) for the combined NMR and UV−vis data. The raw data for the kinetic experiments and the k_{obs} plots are given in the Supporting Information.

Results and Discussion

The complex (1-Me-Ind)(PMe$_3$)Ni−Cl, **2**, was prepared in ca. 40% yield by the direct reaction of (PMe$_3$)$_2$NiCl$_2$

(8) *CAD-4* Software, version 5.0; Enraf-Nonius: Delft, The Netherlands, 1989.
(9) Gabe, E. J.; Le Page, Y.; Charlant, J.-P.; Lee, F. L.; White, P. S. *J. Appl. Crystallogr.* **1989**, *22*, 384.
(10) *SMART*, Release 5.059; Bruker Molecular Analysis Research Tool; Bruker AXS Inc.: Madison, WI 53719-1173, 1999.
(11) *SAINT*, Release 6.06; Integration Software for Single Crystal Data; Bruker AXS Inc.: Madison, WI 53719-1173, 1999.
(12) Sheldrick, G. M. *SHELXL96*, Program for the Solution of Crystal Structures; University of Gottingen: Germany, 1990.
(13) Sheldrick, G. M. *SHELXS*, Program for the Solution of Crystal Structures; University of Goettingen: Germany, 1997.
(14) Flack, H. D. *Acta Crystallogr.* **1983**, *A39*, 876.

Table 1. Crystal Data, Data Collection, and Structure Refinement of 2 and 3

	2	3
formula	$C_{13}H_{18}ClNiP$	$C_{28}H_{42}ClPNi$
mol wt	299.40	503.746
cryst color	dark red	dark red
cryst habit	block	block
cryst dimens, mm	0.53 × 0.27 × 0.19	0.14 × 0.12 × 0.06
symmetry	orthorhombic	monoclinic
space group	$P2_12_12_1$	$P2_1/c$
a, Å	7.783(2)	13.4028(4)
b, Å	11.904(7)	39.7337(12)
c, Å	15.041(4)	10.3414(3)
α, deg	90	90
β, deg	90	101.8960(10)
γ, deg	90	90
volume, Å^3	1393.5(10)	5389.0(3)
Z	4	8
D(calcd), g cm^{-1}	1.427	1.2418
diffractometer	Nonius CAD-4	Bruker AXS SMART 2K
temp, K	220(2)	298(2)
λ(Cu Kα), Å	1.54056	1.54178
μ, mm^{-1}	4.610	2.587
scan type	*ω*/2*θ* scan	Ω scan
θ_{max}	69.82°	73.19°
h,*k*,*l* range	$-9 \le h \le 9$	$-16 \le h \le 16$
	$-14 \le k \le 14$	$-49 \le k \le 48$
	$-18 \le l \le 18$	$-12 \le l \le 10$
no. of reflns used ($I > 2\sigma(I)$)	2650	10 606
abs corr	integration	multiscan SADABS[12]
T (max, min)	0.48 and 0.24	0.8900 and 0.6983
$R[F^2 > 2\sigma(F^2)]$, $wR(F^2)$	0.0194, 0.0493	0.0630, 0.1474
GOF	1.030	1.007

Table 2. Selected Bond Distances (Å) and Angles (deg) for 1−3

	1	2	3a	3b
Ni−P	2.1782(11)	2.1586(7)	2.1875(10)	2.1897(10)
Ni−Cl	2.1865(10)	2.1898(7)	2.2114(10)	2.1884(10)
Ni−C(1)	2.137(2)	2.1316(18)	2.142(4)	2.146(3)
Ni−C(2)	2.072(2)	2.0511(19)	2.042(4)	2.042(3)
Ni−C(3)	2.026(3)	2.0246(18)	2.039(4)	2.037(3)
Ni−C(3A)	2.308(2)	2.3363(19)	2.388(4)	2.392(3)
Ni−C(7A)	2.351(2)	2.3608(19)	2.403(4)	2.411(3)
C(1)−C(2)	1.403(4)	1.398(3)	1.395(5)	1.403(5)
C(2)−C(3)	1.421(4)	1.423(3)	1.424(5)	1.409(5)
C(3)−C(3A)	1.451(4)	1.461(3)	1.458(5)	1.459(5)
C(3A)−C(7A)	1.417(3)	1.418(3)	1.424(5)	1.417(5)
C(1)−C(7A)	1.458(3)	1.459(3)	1.443(5)	1.456(5)
ΔM−C[a]	0.25	0.27	0.30	0.30
P−Ni−Cl	98.82(4)	95.89(2)	94.22(4)	96.43(4)
C(3)−Ni− Cl	161.51(8)	164.87(6)	161.29(11)	160.92(11)
C(3)−Ni−P	99.33(8)	99.18(6)	104.39(11)	102.57(10)
C(1)−Ni−Cl	95.48(8)	98.21(6)	95.56(10)	94.83(10)
C(1)−Ni−P	165.62(7)	164.81(6)	168.83(11)	168.26(10)
C(1)−Ni−C(3)	66.50(10)	66.93(8)	66.10(14)	66.11(14)

[a] See ref 18 for the definition of ΔM−C and literature values for other indenyl complexes.

and Li(1-Me-Ind),[15] while compounds **3**−**5** were prepared by the ligand exchange reactions between the appropriate phosphine ligand and **1** or **2** (Scheme 1). The characterization of complexes **2**−**5** by NMR spectroscopy was quite straightforward because all complexes showed a singlet resonance in their $^{31}P\{^1H\}$ NMR spectra, while their ^1H NMR spectra matched those obtained for other members of this family of complexes.[4] For example, the $^{31}P\{^1H\}$ NMR spectrum of **2** showed a singlet at ca. −10 ppm, while its ^1H NMR spectrum contained the following signals: two doublets and two triplets between 6.5 and 7.0 ppm attributed to H4/H7 and H5/H6, respectively; a doublet at ca. 6.1 ppm due to H2; a broad singlet at 3.58 ppm due to H3; and two doublets at 1.61 and 0.7 ppm attributed to Me-Ind and

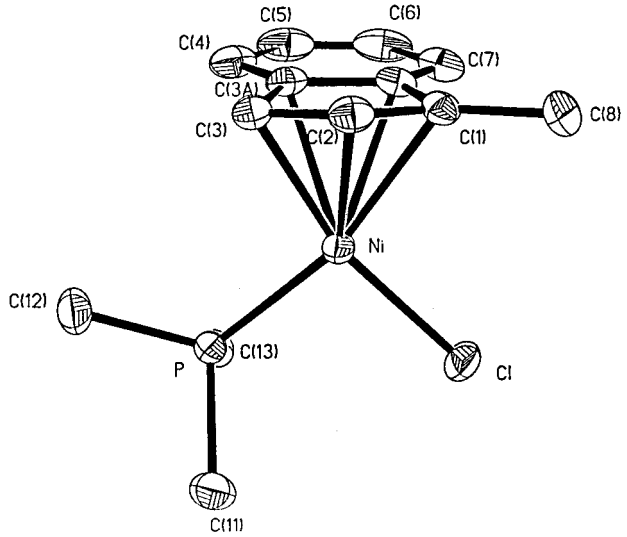

Figure 1. ORTEP diagram for complex **2** showing 30% probability thermal ellipsoids and the atom-numbering scheme.

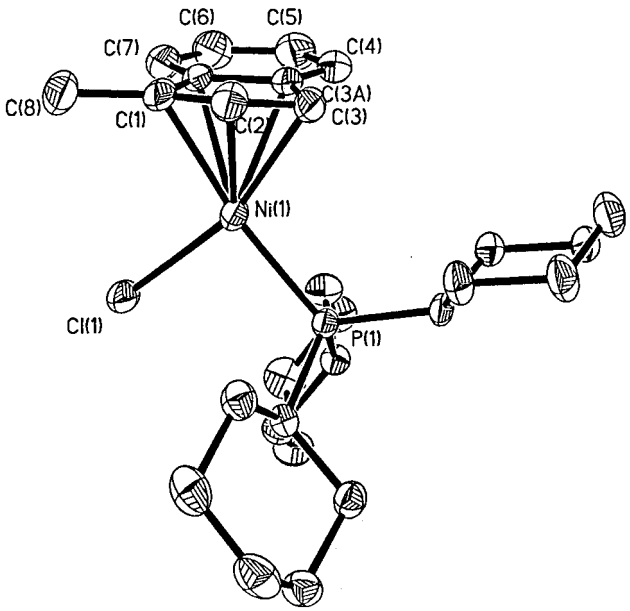

Figure 2. ORTEP diagram for complex **3** showing 30% probability thermal ellipsoids and the atom-numbering scheme. Only one of the two independent molecules present in the unit cell is shown.

(15) (a) The free PMe_3 that is liberated in this reaction can complicate the purification process and reduce the yield if measures are not taken to remove it promptly from the reaction medium. Tests have shown that isolated samples of **2** react with PMe_3 to give $(PMe_3)_2NiCl_2$, $Ni(PMe_3)_4$,[15b] and $(1\text{-Me-Ind})_2$.[15c] We suspect that the coordination of one or more molecules of PMe_3 to the Ni center in **2** leads to the formation of unstable η^1-Ind′ species, which decompose to $(1\text{-Me-Ind})_2$ and $(PMe_3)_3NiCl$; the latter then disproportionates to $Ni(PMe_3)_4$ and $(PMe_3)_2NiCl_2$. (b) The compounds $Ni(PMe_3)_4$ and $(PMe_3)_2NiCl_2$ were identified on the basis of their singlet resonances in the $^{31}P\{^1H\}$ NMR (C_6D_6) spectrum (at ca. −21.3 and −22. 3 ppm for $Ni(PMe_3)_4$ and $(PMe_3)_2NiCl_2$, respectively); in the ^1H NMR spectrum, the complexes can be distinguished on the basis of the doublet resonances for the PMe_3 ligands (at 1.15 and 0.93 ppm for $Ni(PMe_3)_4$ and $(PMe_3)_2NiCl_2$, respectively): Tolman, C. A.; Seidel, W. C.; Gosser, L. W. *J. Am. Chem. Soc.* **1974**, *96*, 53. (c) $(1\text{-Me-Ind})_2$ was identified by comparing its ^1H NMR spectrum to the literature reports: Nicolet, P.; Sanchez, J.-Y.; Benaboura, A.; Abadie, M. J. M. *Synthesis* **1987**, 202.

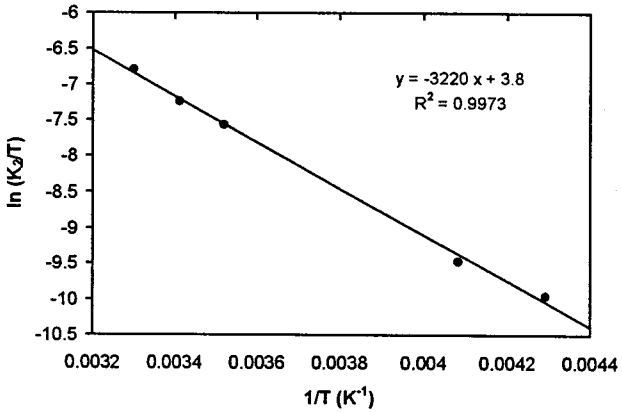

Figure 3. Eyring plot for the reaction of **1** with PCy_3. The K_2 values ($\times 10^{-2}$ M^{-1} s^{-1}): 1.1 ± 0.1 at 233 K; 1.9 ± 0.4 at 245 K; 15 ± 2 at 284 K; 21 ± 2 at 293 K; and 34 ± 7 at 303 K. The activation parameters: $\Delta H^{\ddagger} = 6.40 \pm 0.07$ kcal/mol; $\Delta S^{\ddagger} = -40 \pm 4$ eu.

Scheme 1

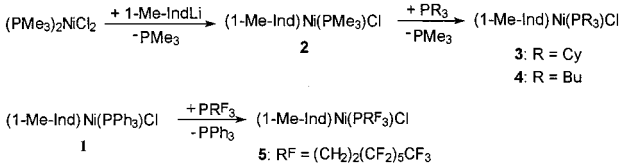

PMe_3, respectively. In addition, complex **5** displayed $^{19}F\{^1H\}$ signals corresponding to the $(CF_2)_5CF_3$ moieties.

Solid State and Solution Hapticities of the 1-Me-Ind Ligand. The solid state structures of complexes **2** and **3** have been studied and compared to that of the previously reported PPh_3 analogue **1** with a view to evaluating the influence of the phosphine ligand on the structures of these complexes. The ORTEP diagrams for **2** and **3** are shown in Figures 1 and 2, while the crystal data and selected bond distances and angles are presented in Tables 1 and 2, respectively. The unit cell of complex **3** contains two independent molecules related to each other by the orientation of the Cy groups in the PCy_3 ligand.[16] The main features of these structures are described below.

If the 1-Me-Ind ligand in complexes **2** and **3** can be considered to be occupying two coordination sites (vide infra), the geometry around the Ni center is approximately square planar, the largest distortion arising from the small C1−Ni−C3 angle of ca. 66°. The Ni−P distance is longer in complex **3** (av 2.188 Å) relative to **2** (2.159 Å; Δ(Ni−P) ≈ 30 σ) presumably because of the much larger cone angle of PCy_3. The 1-Me-Ind ligand in both **2** and **3** is bound to the Ni center primarily through the C1, C2, and C3 atoms (Ni−C(1−3) = 2.02−2.15 Å), whereas the Ni−C3a and Ni−C7a distances are significantly longer (2.33−2.41 Å). This "slippage" away from an ideal η^5 hapticity is commonly observed in this family of complexes[4] and can be attributed to the tendency of a Ni(II) center to avoid forming 18-electron complexes.[17] The parameter ΔM−C = {M−C_{av} (for C3a,-

Chart 1

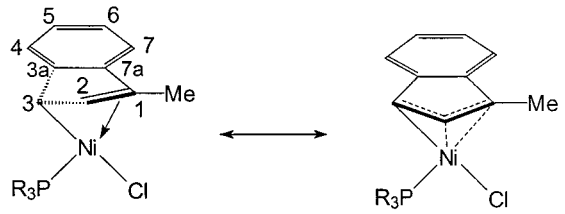

7a) − M−C_{av} (for C1,3)} is often used to measure the extent to which Ind ligands have slipped away from the ideal η^5 hapticity wherein ΔM−C should be nearly zero.[18] The ΔNi−C values for **3** (0.30 Å) and **2** (0.27 Å) are somewhat larger than those observed for complex **1** (0.25 Å), reflecting the stronger nucleophilicity of the tri(alkyl) phosphines.

Another commonly observed feature in these complexes is the unequal Ni−C1 and Ni−C3 bond distances (Ni−C1 > Ni−C3 in **2** and **3**, ΔNi−C is ca. 25−50 σ); this type of "sideways slippage" can be attributed to the unequal trans influences of the PR_3 and Cl ligands. Therefore, we propose that the 1-Me-Ind ligand in complexes **1**−**3** adopts solid state hapticities that can best be denoted as $\eta^5 \leftrightarrow \eta^3 \leftrightarrow \eta^1,\eta^2$ (Chart 1). Clark et al. have put forth a similar mode of bonding, namely, $\eta^3 \leftrightarrow \eta^1,\eta^2$, for the allyl ligand in the complexes (η-C_3H_5)-Pt(PR_3)X on the basis of solution NMR data.[19]

The solid state data described above suggest that complexes **1**−**3** have very similar structures in the solid state, and it is unclear whether the subtle structural differences observed (e.g., different ΔNi−C values) might be responsible for the differences in the catalytic activities of complexes **2** and **3** compared to **1**.[7] Given that the solution structures of complexes **1**−**3** are more likely to affect their reactivities, we have compared below some of the structural features of these complexes as gleaned from their solution $^{13}C\{^1H\}$ NMR spectra.

The solution hapticity of an indenyl ligand in a given complex may be estimated by using the equation $\Delta\delta_{av}C = \delta_{av}$(C3a, 7a of η-Ind) − δ_{av}(C3a, 7a of Na^+ Ind^-) to compare the $^{13}C\{^1H\}$ NMR chemical shifts of the C3a and C7a nuclei in that complex to the corresponding shifts in Na^+Ind^-, for which the Ind hapticity is considered to be intermediate between η^5 and η^3.[18a] According to this protocol, the solution hapticity of the Ind ligand is thought to be closer to η^5 when $\Delta\delta_{av}C \ll 0$ (e.g., $\Delta\delta_{av}C$ for Ind_2Fe is ca. −42 ppm),[18a] closer to η^3 when $\Delta\delta_{av}C \gg 0$ (e.g., $\Delta\delta_{av}C$ for (Ind)Ir(PMe_2Ph)$_3$ is ca. +28 ppm),[18a] or intermediate when $\Delta\delta_{av}C \approx 0$ (e.g., $\Delta\delta_{av}C$ for $(Ind)_2Ni$ is ca. +5 ppm).[18b] The $\Delta\delta_{av}C$ values for complexes **1**−**5** are ca. −2 ppm for **1**, **2**, and **4** and ca. −1 ppm for **3** and **5**, implying an intermediate ($\eta^5 \leftrightarrow \eta^3$) hapticity for the 1-Me-Ind ligand in all of these complexes. The similarity of the $\Delta\delta_{av}C$ values indicates that the solution hapticity of the 1-Me-Ind ligands in these complexes is also very similar; therefore, structural factors alone cannot explain the differences in the

(16) We thank a reviewer for pointing out that a similar situation exists in the solid state structure of complex (1-Me-Ind)Rh(η^2-C_2H_4)(PCy_3): Westcott, S. A.; Kakkar, A. K.; Taylor, N. J.; Roe, D. C.; Marder, T. B. *Can. J. Chem.* **1999**, *77*, 205.

(17) For a detailed discussion of hapticity issues in the corresponding CpNi complexes see: Holland, P. L.; Smith, M. E.; Andersen, R. A.; Bergman, R. G. *J. Am. Chem. Soc.* **1997**, *119*, 12815.

(18) For a discussion of the correlations between the solid state and solution hapticities for indenyl complexes, on one hand, and the ΔM−C values and the ^{13}C NMR data, on the other, see: (a) Baker, R. T.; Tulip, T. H. *Organometallics* **1986**, *5*, 839. (b) Westcott, S. A.; Kakkar, A. K.; Stringer, G.; Taylor, N. J.; Marder, T. B *J. Organomet. Chem.* **1990**, *394*, 777.

(19) Clark, H. C.; Hampden-Smith, M. J.; Ruegger, H. *Organometallics* **1988**, *7*, 2085.

observed reactivities between complexes **2** and **3** on one hand and **1** on the other.

Ligand Substitution Reactions. The results of the ethylene polymerization reactions catalyzed by complexes **1**−**3**[6b] raised the question of whether the phosphine ligands in these complexes dissociate prior to the coordination of the incoming substrate molecule, as is thought to be the case with the Grubbs system.[3] Since most square planar d^8 complexes follow an associative mechanism in ligand exchange reactions, the predissociation of the phosphine ligand in complexes such as **1**−**5** would seem unlikely; it should be noted, however, that these compounds might, in principle, undergo a dissociative substitution owing to the flexible hapticity of the Ind′ ligand, which can adjust its electronic contribution to the Ni center by slipping back and forth between the η^3 and η^5 modes. This possibility prompted us to study the mechanism of the phosphine substitution reaction in the title complexes in order to determine whether phosphine dissociation and/or hapticity changes are involved in these reactions.

The choice of a specific substitution reaction for the kinetic studies was made on the basis of the following considerations. The reaction of **1** with PR^F_3 was unsuitable due to the limited solubilities of both PR^F_3 and complex **5**. The rates of the substitution reactions between complex **2** and the other phosphines were too slow for studying, while those for the reactions of **1** with PMe_3 or PBu_3 were too rapid for convenient monitoring. The reaction of **1** with PMe_3 was doubly unsuitable for our purposes because the product of the reaction, complex **2**, reacts further with PMe_3, which is present in excess, to give a number of decomposition products.[15] In contrast, the reaction of **1** with PCy_3 showed a rate profile that was convenient to monitor and did not lead to secondary products; therefore, this reaction was chosen for our kinetic studies.

The pseudo-first-order rate of the reaction of **1** with PCy_3 (10−20-fold excess) at low temperatures was studied by the $^{31}P\{^1H\}$ NMR monitoring of the disappearance of **1** relative to $O{=}PPh_3$.[20] Plots of $\ln([\mathbf{1}]/[\mathbf{1}]_0)$ vs time gave straight lines passing through the origin with slopes of k_{obs}, while plots of the k_{obs} values vs different $[PCy_3]_0$ values (10-, 15-, and 20-fold excess) gave straight lines with slopes of K_2. The rate of the ligand exchange reactions at high termperatures was studied in a similar manner using UV−vis spectroscopy. The activation parameters $\Delta H^{\ddagger}$ (6.40 ± 0.07 kcal/mol) and $\Delta S^{\ddagger}$ (−40 ± 4 eu) were obtained from a plot of $\ln(K_2/T)$ vs $1/T$ (Figure 3).

The results of the kinetic studies, namely, the clear dependence of the rate on the $[PCy_3]$ and the negative value of $\Delta S^{\ddagger}$, imply that the phosphine substitution reaction for complex **1** follows an associative mechanism. Consistent with this supposition, we found that steric factors exert great influence on the rate of this ligand exchange reaction; thus, the substitution of PPh_3 by PCy_3 proceeds 100−1000 times more slowly for the more sterically encumbered complex (1-Me,2-Ph-Ind)-Ni(PPh_3)Cl (exchange takes hours at room temperature). On the other hand, when a similar experiment was carried out with the less bulky Cp analogue CpNi-(PPh_3)Cl, we observed that the substitution of PPh_3 by PCy_3 was essentially over in the time of mixing even at 233 K, i.e., the exchange rate is 10−100 times more rapid for the Cp analogue. The latter result not only confirms the importance of the steric factors but also implies that hapticity changes cannot play an important role in these ligand exchange reactions since Cp complexes would be expected to be less apt to undergo such slippage than their Ind′ analogues. We conclude, therefore, that the ligand exchange reaction with complex **1** follows an associative mechanism and likely involves the formally five-coordinate, 18-electron[21] intermediate or activated complex **I** shown in Scheme 2.

Scheme 2

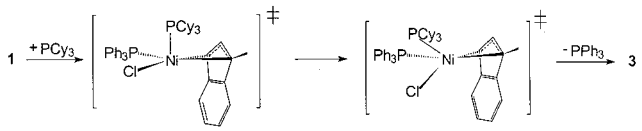

It is noteworthy that five-coordinate intermediates of the type (π-allyl)NiL_2R have also been postulated in a number of other catalytic reactions,[22] while many five-coordinate d^8 compounds have been shown to be relatively stable species.[23] Although the isolation of formally five-coordinate, 18-electron complexes such as **I** has eluded us so far, we have obtained spectroscopic evidence for the existence (in solution) of a closely related analogue wherein the incoming L ligand is tethered

(20) Tests have shown that $O{=}PPh_3$ is completely unreactive toward both the starting material and the product in these reactions.

(21) We propose that the 1-Me-Ind ligand occupies two coordination sites in the intermediate **I** as opposed to slipping into an η^1 mode, because the formation of η^1-Ind′ derivatives in this family of compounds normally leads to decomposition involving the coupling of the Ind′ ligands (refs 4d and 15). Moreover, if slippage into an η^1 mode were required, the ligand exchange reaction would be expected to proceed more slowly for the Cp analogue, whereas the opposite was observed. However, a reviewer has pointed out that this conclusion may not be warranted in view of the fact that the $CpNiL_n$ systems do not display the same type of hapticity changes as the analogous Ind complexes. For example, the paramagnetic complex Cp*Ni(acac)(PMe_3), which would be formally considered a 20-electron complex, does not show any "slippage" but rather an overall lengthening of the Ni−C(Cp*) bonds (Smith, M. E.; Andersen, R. A. *J. Am. Chem. Soc.* **1996**, *118*, 11119). A similar behavior is seen when comparing the structural features of Cp_2M vs Ind_2M complexes (M = Fe, Co, Ni): the Cp complexes retain the 5-fold axis as the electron count goes from 18 to 19 to 20, but the M−C distances increase; on the other hand, the corresponding Ind analogues undergo slip-fold distortions whose degrees increase with the increasing electron count (ref 18b). Therefore, in terms of their coordination to Ni, the Cp and Ind ligands seem to respond differently to changes in the electronic environment around Ni, so that it may be possible for the Cp and Ind complexes to both undergo associative ligand exchange. In the Cp case, the association of the incoming PCy_3 would result in longer Ni−Cp distances without causing hapticity changes, whereas in the Ind case there would be subtle hapticity changes. We thank this reviewer for bringing this different interpretation to our attention.

(22) (a) Bosnich, B.; Mackenzie, P. B. *Pure Appl. Chem.* **1982**, *54*, 189. (b) Cherest, M.; Felkin, H.; Umpleby, J. D.; Davies, S. G. *J. Chem. Soc., Chem. Commun.* **1981**, 681. (c) Consiglio, G.; Piccollo, O.; Roncetti, L.; Morandini, F. *Tetrahedron* **1986**, *42*, 2043. (d) Kurosawa, H. *J. Organomet. Chem.* **1987**, *334*, 243.

(23) (a) For a few trigonal bipyramidal compounds of d^8 metals with tripodal tetradentate ligands see: Aizawa, S.-i.; Ilida, T.; Funahashi, S. *Inorg. Chem.* **1996**, *35*, 5163, and the references therein. (b) For a few five-coordinate complexes of Rh(I) with multidentate imine ligands see: Haarman, H. F.; Bregman, F. R.; Ernsting, J.-M.; Veldman, N.; Spek, A. L.; Vrieze, K. *Organometallics* **1997**, *16*, 54, and the references therein. (c) For square pyramidal Pd(II) complexes of the type $(PR_3)_3$-PdX_2 see: Louw, W. J.; de Waal, D. J. A.; Kruger, G. J. *J. Chem. Soc., Dalton Trans.* **1976**, 2364. Collins, J. W.; Mann, F. G.; Watson, D. G.; Watson, H. R. *J. Chem. Soc.* **1964**, 1803. (d) For a trigonal bipyramidal ethylene complex of Pt(II) see: Maresca, L.; Natile, G.; Calligaris, M.; Delise, P.; Randaccio, L. *J. Chem. Soc., Dalton Trans.* **1976**, 2386.

to the Ind, namely, (η^3,η^1-Ind$CH_2CH_2-NMe_2$)Ni(PPh_3)Cl:[24]

(η^3,η^0-Ind$CH_2CH_2-NMe_2$)Ni(PPh_3)Cl ⇌ (η^3,η^1-Ind$CH_2CH_2-NMe_2$)Ni(PPh_3)Cl

Conclusion. The structural studies outlined in this report have not revealed significant differences in the hapticity of the 1-Me-Ind ligand to account for the different reactivities of complexes **1**−**3**. Thus, the solid state hapticities are somewhat different in these complexes, but the solution hapticities are virtually identical. The Ni−P bond length in **1** is intermediate between the shorter distance in **2** and the longer one in **3**, while the order of ethylene polymerization activities is **2** ∼ **3** > **1**.

The kinetic studies indicate that five-coordinate intermediates such as **I** (Scheme 2) are likely involved in the phosphine substitution reactions. The species **I** is analogous to the proposed[6] intermediates for the polymerization of Ph−CC−H and ethylene, namely, (Ind′)(PR_3)Ni(X)(L), with L being a substrate molecule such as ethylene and X being the growing polymer chain.[25] Although substrates such as ethylene are less nucleophilic than PCy_3, they are also significantly less bulky and present in very large excess compared to PCy_3. It is, therefore, tempting to suppose that this type of associatively activated intermediates play a major role in the polymerization reactions catalyzed by our complexes. We recognize, however, that the presence of a large excess of Lewis acids such as MAO in the catalytic settings might render the normally unfavorable dissociation of PR_3 more plausible. To be sure, NMR monitoring of the reaction of **1** with 50−100 equiv of MAO failed to detect the formation of the MAO·PPh_3 adduct, although this cannot rule out the possibility that under the catalytic conditions (i.e., 500 equiv of MAO) small amounts of a highly active species are generated via phosphine dissociation.

(24) Groux, L. F.; Bélanger-Gariépy, F.; Zargarian, D.; Vollmerhaus, R. *Organometallics* **2000**, *19*, 1507.

(25) We have proposed that the reaction of this intermediate with PMAO-type cocatalysts would serve to weaken the Ni−X bond (without ionizing it), thus facilitating the insertion of ethylene (ref 6b).

Acknowledgment. The Natural Sciences and Engineering Research Council of Canada and FCAR of Québec are gratefully acknowledged for financial support. We are also indebted to Dr. I. Horvath for the generous gift of a sample of P{$(CH_2)_2(CF_2)_5CF_3$}$_3$, Dr. R. Vollmerhaus for carrying out some of the initial experiments on the synthesis of **2**, Prof. D. Macartney for help with the UV−vis studies, and Prof. S. Collins for many stimulating discussions on the mechanism of the polymerization reactions in our system.

Supporting Information Available: Complete details of the X-ray analysis of **2** and **3**, including tables of crystal data, collection and refinement parameters, bond distances and angles, anisotropic thermal parameters, and hydrogen atom coordinates; tables of the raw data for the kinetic study. This material is available free of charge via the Internet at http://pubs.acs.org.

OM010608W